

# AN ANALYSIS OF PARAMETERS AFFECTING SLAPDOWN OF TRANSPORTATION PACKAGES\*

V. L. Bergmann  
D. J. Ammerman  
Sandia National Laboratories  
Albuquerque, New Mexico

## ABSTRACT

Several parameters affecting the accelerations experienced by packages for the transport of nuclear material during eccentric impact are evaluated. Eccentric impact on one end of a cask causes rotation leading to secondary impact, referred to as slapdown, at the other end. In a slapdown event, the rotational acceleration during the primary impact can cause accelerations at the nose and tail which are greater than those during a side-on impact. Slapdown can also cause acceleration at the tail during the secondary impact to be more severe than at the nose during primary impact. Both of these effects are investigated for two cask geometries. Other parameters evaluated are the characteristics of impact limiters and friction between the impact limiter and the impacted surface. Results were obtained using SLAPDOWN, a code which models the impact response of deformable bodies.

## INTRODUCTION

In the certification of packages for transport of radioactive material, the issue of slapdown must be addressed. Slapdown is secondary impact resulting from rotational acceleration imparted to the cask during eccentric primary impact. In a previous report (1), Sjaardema and Wellman developed the computer code, SLAPDOWN, to model slapdown behavior. They investigated several effects of geometry, impact limiter models, friction, and scaling behavior. Slapdown severity was measured by the ratio of tail to nose velocities and by the displacement of the springs representing impact limiter behavior. In this paper, we further examine the effects of friction, in particular, its influence on the behavior of different geometries and impact limiter models. Our purpose is to re-emphasize the need to consider secondary impact events during cask design. Because cask designers are interested in the accelerations experienced by a cask during impact, acceleration is used as the measure of slapdown severity.

Even though the casks studied here have the same geometry at both ends, the terms nose and tail will be used to designate the ends which impact first and second, respectively. The term primary impact will be used to designate time during which the nose is in contact with the impacted surface, while secondary impact will refer to the event of tail impact. Peak nose and tail accelerations are computed during both primary and secondary impacts.

## METHOD OF ANALYSIS

In SLAPDOWN (1), a transportation cask is modeled as a rigid bar with springs attached at the ends (Fig. 1) to simulate the behavior of the impact limiters. Spring behavior may be either elastic or inelastic, and can be nonlinear.

The motion of the bar is computed from the equations of planar rigid body dynamics (2),

$$\vec{F} = m\vec{a}_{CG} \quad (\text{Eq. 1})$$

$$M_{CG} = I_{CG} \alpha \quad (\text{Eq. 2})$$

In the first equation,  $\vec{F}$  is the total force vector applied to the body,  $m$  is the mass of the body, and  $\vec{a}_{CG}$  is the acceleration of the center of gravity (CG). In Eq.(2),  $M_{CG}$  is the moment of the external forces about the CG,  $I_{CG}$  is the mass moment of inertia about the CG, and  $\alpha$  is the angular acceleration of the body. It must be noted that the relationship of Eq.(1) applies only to the acceleration at the CG, and is not valid in general for acceleration at any other point on the body. From planar kinematics, the vertical component of the acceleration at any point,  $\ddot{y}$ , on a rigid body is given by,

$$\ddot{y} = \ddot{y}_{CG} + \alpha l \cos \theta + \omega^2 l \sin \theta \quad (\text{Eq.3})$$

where  $\ddot{y}_{CG}$  is the vertical component of acceleration at the CG,  $\theta$  is the instantaneous angle between the axis of the body and the horizontal,  $\dot{\theta}$  is the angular velocity, and  $\omega$  is the distance from the center of gravity to the point. We consider only the vertical component of acceleration because the horizontal component is much smaller for shallow angle impacts. Equation (3) is based on the positive directions for  $x$ ,  $y$ , and  $\theta$  defined in Fig. 1. The equations of rigid body motion indicate that a force whose line of action does not pass through the center of gravity has two effects on the motion of a rigid body. It causes translational acceleration of the CG and angular acceleration of the rigid body.

Accelerations for an example impact are shown in Fig. 2. Because the nose is assumed to be at the left end ( $l_n$  is negative), initial impact imparts a negative angular acceleration to the cask. Thus, the nose acceleration is greater than that at CG, while the tail ( $l_t$  is positive) acceleration is less

\* This work performed at Sandia National Laboratories, Albuquerque, New Mexico, supported by the U.S. Department of Energy under Contract DE-AC04-76DP00789.

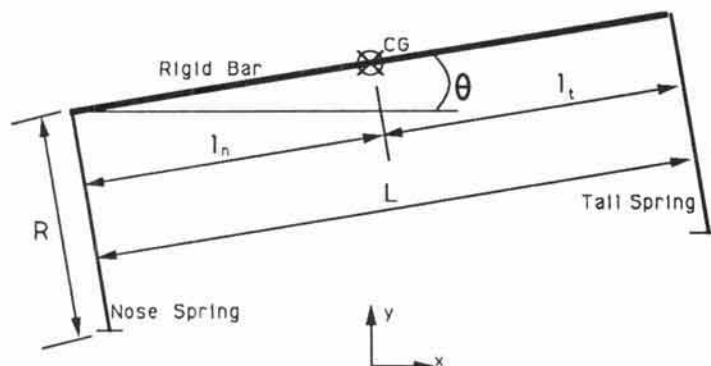


Fig. 1. Model used in SLAPDOWN code.

than the CG. Later, when the tail hits, the angular acceleration becomes positive. Therefore, during secondary impact the nose acceleration is less than that of the center of gravity and the tail acceleration is greater.

**RESULTS OF PARAMETER SENSITIVITY ANALYSIS**

The slapdown behavior of two different cask geometries with the properties shown in Table I was examined using a coefficient of friction of 0.2. The CG was assumed to lie at the center of each cask, and the nose and tail impact limiters were assumed to be identical. For the elastic spring model of the impact limiters, a spring stiffness of 3500 MN/m was used. The nonlinear, inelastic spring models had the force deflection curve shown in Fig. 3. Unloading was assumed to be along a path parallel to the initial loading stiffness. Thus, during large inelastic deformation of the springs, most of the energy is dissipated by the spring and very little is recovered upon unloading.

Figure 4 shows the effect of the length to radius of gyration ratio ( $L/r$ ) on peak nose and tail accelerations when the impact limiters are modeled as elastic springs. On this plot and all subsequent plots, each data point represents

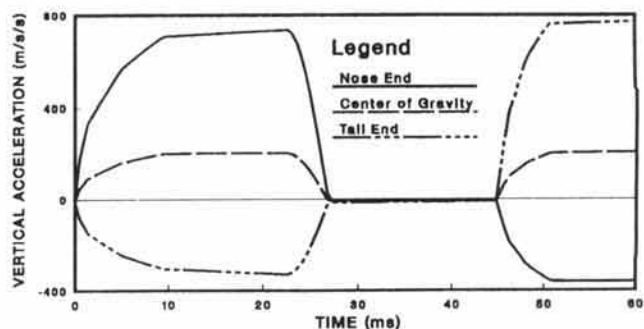


Fig. 2. Vertical acceleration along the cask axis during oblique impact of a cask with  $L/r = 3.3$ ,  $\mu = 0$ .

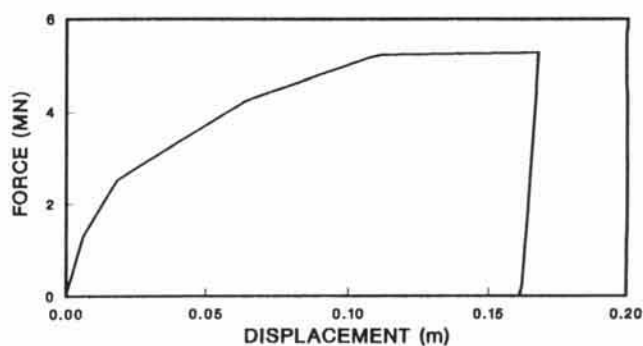


Fig. 3. Force displacement relationship for inelastic spring model.

**TABLE I**

Cask Properties

Cask	Mass $m$ (kg)	Moment $I$ ( $\text{kg} \cdot \text{m}^2$ )	Total Length $L$ (m)	Radius of Gyration $r$ (m)	$L/r$	Impact Limiter Radius $R$ (m)
1	13,480	6,550	1.40	.696	2.0	1.07
2	24,860	55,370	4.88	1.49	3.3	1.14

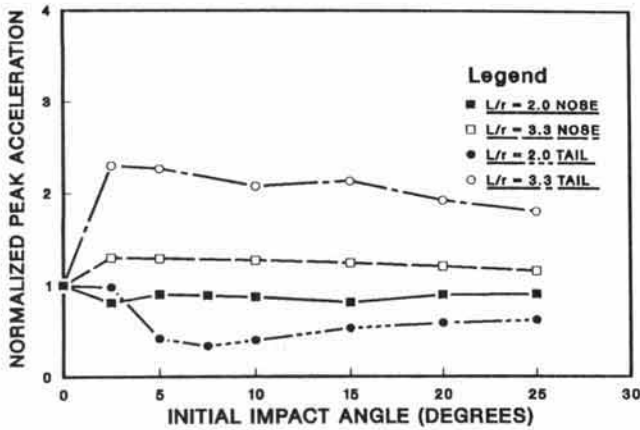


Fig. 4. Effect of  $L/r$  on normalized peak nose and tail accelerations for elastic spring model of impact limiters.

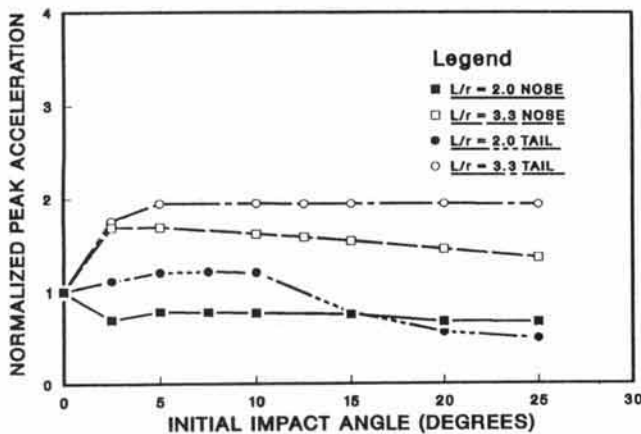


Fig. 5. Effect of  $L/r$  on normalized peak nose and tail accelerations for inelastic spring model of impact limiters.

a run of the SLAPDOWN code for that particular initial impact angle. Peak acceleration is the maximum acceleration experienced during the entire impact event. To isolate the effect of the  $L/r$  ratio from the effects of mass and spring characteristics, accelerations have been normalized with respect to the side drop acceleration for each case. For the cask with  $L/r = 2$ , neither the nose nor the tail accelerations exceed the side drop accelerations for any of the initial

impact angles. Furthermore, except for one point at  $2.5^\circ$ , the peak tail accelerations do not exceed peak nose accelerations. For the cask with  $L/r$  equal to 3.3, nose and tail accelerations are higher than the side drop accelerations, with the maximum occurring at an initial impact angle of  $2.5^\circ$ . For this case, peak tail accelerations occurring during secondary impact are significantly higher than nose accelerations occurring during primary impact.

Peak accelerations for the casks when the impact limiters are modeled as inelastic springs are shown in Fig. 5. The side drop accelerations used for normalization are much less than for the elastic spring model. Thus, the actual accelerations calculated for a cask using an inelastic model for the impact limiters are much less than those computed for elastic spring models. However, examination of the normalized peak accelerations reveals some interesting trends. For the cask with  $L/r = 2$ , the nose accelerations are again always less than the acceleration during side-on impact. For initial impact angles less than  $15^\circ$ , peak tail accelerations exceed both the peak nose accelerations and the side drop acceleration. This effect is probably due to the presence of friction at both the nose and tail. Friction at the nose during primary impact causes rotational acceleration opposite to the direction caused by the normal force, thus decreasing the peak nose acceleration. However, during secondary impact, the friction at the tail tends to cause rotational acceleration in a direction that adds to that caused by the normal force at the tail. Therefore, friction at the tail increases the accelerations at the tail during secondary impact.

For the cask with  $L/r = 3.3$ , the normalized peak nose acceleration is greater for the inelastic model, while the peak tail acceleration is less than the normalized accelerations for the elastic model. However, both are still greater than the side impact accelerations, and the peak tail accelerations during secondary impact are higher than the nose acceleration during primary impact. Thus, even when energy-absorbing, inelastic models are used for the impact limiters, slapdown must be considered.

The effects of the friction force on peak accelerations are further examined in Figs. 6 through 11. Both the magnitude and the point of application of the friction force influence the accelerations of a cask. The effect of the magnitude of the friction is analyzed by varying the coefficient of friction. The effect of the point of application is examined by using different impact limiter radii. As the radius of the impact limiter increases, the distance from the point of application of the friction force and the CG increases. Thus, the moment and the angular acceleration imparted to the cask by the friction force both increase.

Figures 6 through 9 show the effect of varying the coefficient of friction on peak nose and tail accelerations for the two casks with inelastic impact limiters. As shown in Fig.

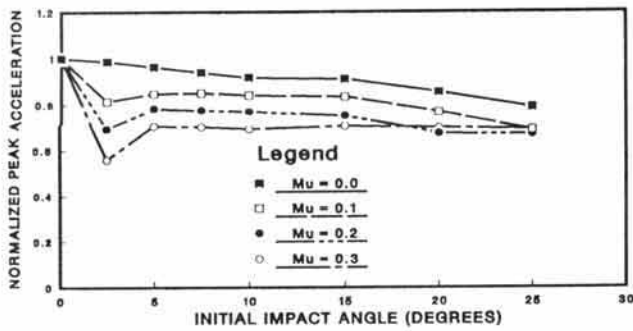


Fig. 6. Effect of the coefficient of friction on peak nose accelerations for a cask with  $L/r = 2.0$ . (Accelerations normalized with respect to the side drop acceleration of 767 m/s/s.)

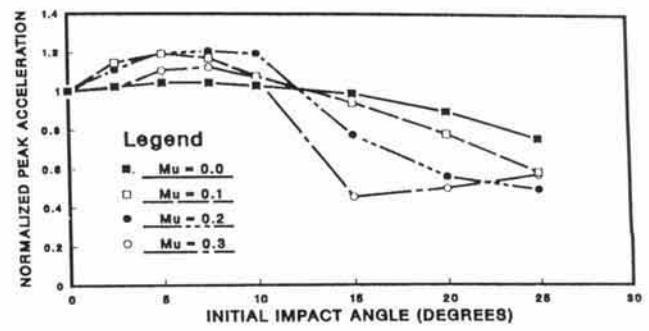


Fig. 8. Effect of the coefficient of friction on peak nose accelerations for a cask with  $L/r = 3.3$ . (Accelerations normalized with respect to the side drop acceleration of 419 m/s/s.)

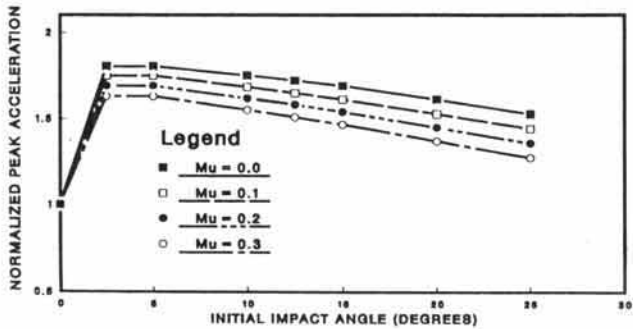


Fig. 7. Effect of the coefficient of friction on peak tail accelerations for a cask with  $L/r = 2.0$ . (Accelerations normalized with respect to the side drop acceleration of 767 m/s/s.)

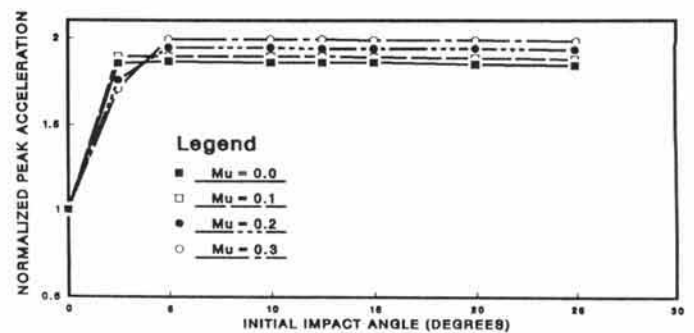


Fig. 9. Effect of the coefficient of friction on peak tail accelerations for a cask with  $L/r = 3.3$ . (Accelerations normalized with respect to the side drop acceleration of 419 m/s/s.)

6, the peak nose acceleration for the cask with  $L/r = 2$  does not exceed the side drop acceleration for any of the coefficients of friction analyzed. Furthermore, an increase in the friction force tends to decrease peak nose accelerations. On the other hand, the corresponding results for tail acceleration in Fig. 7 show an increase in peak tail accelerations with increasing friction at low initial impact angles for this cask. These results are consistent with the above discussion of the effects of friction at the nose and tail. Furthermore, at initial impact angles less than  $15^\circ$ , the tail hits while the nose is still in contact with the impacted surface. With both the nose and tail in contact simultaneously the translational acceler-

ation of the CG is higher and thus contributes to a higher tail acceleration at low initial impact angles.

Figure 8 shows the effect of varying the magnitude of the friction force on the peak nose acceleration for the more slender cask ( $L/r = 3.3$ ). Here, an increase in friction force clearly causes a reduction in the peak nose accelerations at all initial impact angles analyzed. Conversely, the maximum peak tail acceleration over the range of initial impact angles examined increases with increasing friction coefficient (Fig. 9). An increase in friction also tends to increase the initial impact angle at which the maximum tail acceleration occurs. For the smaller two values of the friction coefficient, the maximum tail acceleration occurs at an impact angle of  $2.5^\circ$ ,



but the maximum acceleration for the higher values of friction does not occur until 5°.

Finally, the effect of the point of application of the friction force is analyzed by examining the response with three different impact limiter radii. In these calculations, an  $L/r$  of 3.3 and a friction coefficient of 0.2 was assumed. An increase in the radius of the impact limiter causes a decrease in peak nose accelerations (Fig. 10), and an increase in peak tail accelerations (Fig. 11). These results are similar to the effects of increasing the magnitude of the friction force shown in Figs. 7 and 8. However, in this case the effect is due to changing the moment arm of the friction force rather than the magnitude.

SUMMARY

Several design parameters have been examined for their effect on slapdown severity for radioactive material transportation packages. In particular, the effects of friction on these parameters has been investigated. Results indicate that the cask with an aspect ratio greater than 2 has nose and tail accelerations greater than the side drop acceleration at all values of friction considered. Furthermore, the tail accelerations during secondary impact are higher than nose accelerations during primary impact. Finally, an increase in the friction force or in the corresponding moment about the center of gravity decreases peak nose accelerations and increases peak tail accelerations.

For a cask with  $L/r = 2$ , peak nose accelerations for all values of friction and initial impact angles are less than the side drop acceleration. However, in the presence of friction, the peak tail accelerations are greater than the side drop acceleration at impact angles less than 10°. Therefore, even casks with low aspect ratios can exhibit slapdown behavior if friction is assumed to act at both the nose and tail impact limiters.

All of the computations presented in this paper were performed assuming the initial horizontal velocity of the cask was zero. Because the direction of the friction is always opposite to the direction of motion at the impact point, an initial horizontal velocity could greatly affect the influence of friction on the peak accelerations. If the direction of friction is reversed, the direction of the moment and angular acceleration due to friction will be reversed. Although this will not influence the vertical acceleration of the center of gravity, it will affect the vertical accelerations of the nose and tail. These effects need to be examined to more fully characterize the influence of friction on slapdown behavior.

REFERENCES

1. G. D. SJAARDEMA and G. W. WELLMAN, "Numerical and Analytical Methods for Approximating the Ec-

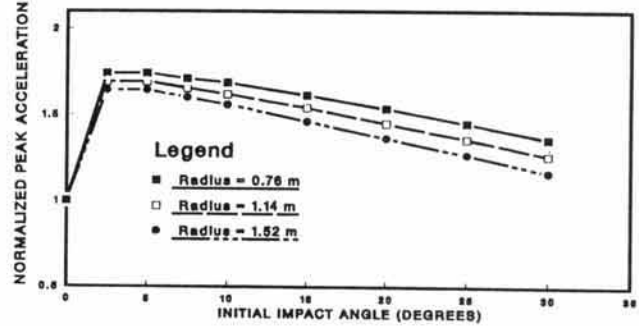


Fig. 10. Effect of impact limiter radius on peak nose accelerations for a cask with  $L/r = 3.3$ ,  $\mu = 0.2$ . (Accelerations normalized with respect to the side drop acceleration of 419 m/s/s.)

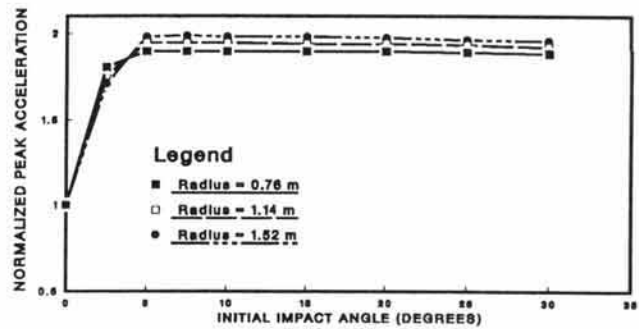


Fig. 11. Effect of impact limiter radius on peak tail accelerations for a cask with  $L/r = 3.3$ ,  $\mu = 0.2$ . (Accelerations normalized with respect to the side drop acceleration of 419 m/s/s.)

entric Impact Response (Slapdown) of Deformable Bodies," SAND88-0616, Sandia National Laboratories, Albuquerque, NM, March 1988.

2. F. P. BEER and E. R. JOHNSTON, JR., Vector Mechanics for Engineers: Dynamics, Third Edition, McGraw-Hill Book Company, 1977.